Design, synthesis, biological and *in silico* evaluation of 3-carboxy-coumarin sulfonamides as potential antiproliferative agents targeting HDAC6

JOSÉ L. MADRIGAL-ANGULO[1], GUSTAVO A. HERNÁNDEZ-FUENTES[2,3], HORTENSIA PARRA-DELGADO[1], MARYCRUZ OLVERA-VALDÉZ[4], ITZIA I. PADILLA-MARTÍNEZ[4], ARIANA CABRERA-LICONA[3], ALEXANDRA S. ESPINOSA-GIL[2], IVAN DELGADO-ENCISO[2,3] and FRANCISCO J. MARTÍNEZ-MARTÍNEZ[1]

[1]Faculty of Chemical Sciences, University of Colima, Coquimatlán 28400, Mexico; [2]Department of Molecular Medicine, School of Medicine, University of Colima, Colima 28040, Mexico; [3]State Cancerology Institute of Colima, Health Services of The Mexican Social Security Institute for Welfare (IMSS-BIENESTAR), Colima 28085, Mexico; [4]Laboratorio de Química Supramolecular y Nanociencias, Unidad Profesional Interdisciplinaria de Biotecnología, Instituto Politécnico Nacional, Ciudad de México 07340, Mexico

Received May 21, 2024; Accepted October 2, 2024

DOI: 10.3892/br.2024.1884

Abstract. Breast cancer (BC) is the most common cancer and the main cause of mortality due to cancer in women around the World. Histone deacetylase 6 (HDAC6) is a promising target for the treatment of BC. In the present study, a series of novel 3-carboxy-coumarin sulfonamides, analogs of belinostat, targeting HDAC6 were designed and synthesized. The compounds were synthesized and purified through open-column chromatography. Characterization was performed using spectroscopic techniques, including ^{1}H and ^{13}C NMR, homonuclear and heteronuclear correlation experiments, IR and UV. Molecular docking was carried out using AutoDock Vina implemented in UCSF Chimera version 1.16 against the HDAC6 protein structure (PDB: 5EDU). 2D protein-ligand interaction diagrams were generated with Maestro, and validation was conducted by redocking trichostatin A into the HDAC6 active site. Additionally, the compounds were evaluated in cancer cell lines (MDA-MB-231, MCF-7 and NIH/3T3), and healthy cells using lymphocytes from healthy volunteers. In the *in vitro* experiments, the compounds evaluated showed cytotoxic activity against the BC cell lines MCF-7 and MDA-MB-231 and the non-malignant cells 3T3/NIH. Compounds 5, 8a-c exhibited antiproliferative activity comparable to that of cisplatin and doxorubicin. Molecular docking studies showed that compounds with the 3-benzoylcoumarin scaffold had favorable affinity with catalytic domain of HDAC6 and whose interactions are similar to those found in belinostat. Compounds 5, 8b, 8c, 4c, and 8a exhibited higher viability against nonmalignant cells (leukocytes), with percentages ranging from 73-87%, demonstrating 3-4-fold lower potency than belinostat against healthy cells.

Correspondence to: Dr Francisco J. Martínez-Martínez, Faculty of Chemical Sciences, University of Colima, Km 9 Coquimatlán-Colima Highway, Coquimatlán 28400, Mexico
E-mail: fjmartin@ucol.mx

Key words: 3-carboxy-coumarin sulfonamides, histone deacetylase inhibitors, molecular docking, *in silico* analysis, triple-negative breast cancer

Introduction

Breast cancer (BC) is a complex and heterogeneous disease characterized by abnormal cell proliferation of the epithelial cells lining the milk ducts (1). BC is the most common cancer and the main cause of mortality due to cancer in women globally, with an age-standardized incidence rate (world) of 46.8 per 100,000 and a mortality rate of 12.7 per 100,000 for both sexes, as reported in the most recent data (2). There is a wide variety of drugs for the pharmacological treatment of BC. However, most drugs act directly on DNA with severe adverse effects (3). Histone deacetylase (HDAC) inhibitors are a promising new class of anticancer drugs, which indirectly modifies the expression of genes (4).

HDACs are zinc-dependent enzymes that remove acetyl groups from lysine and arginine residues in histone proteins on DNA leading to chromatin compaction and therefore transcription repression (5). Overexpression of HDACs has been reported in numerous cancer types and is directly linked to accelerated cell proliferation and survival (6). There are 18 isoforms identified in humans and the overexpression of isoform HDAC-6 has been correlated with BC (7). HDAC inhibitors have been successfully used in the treatment numerous types of cancer inducing cell cycle arrest, activating extrinsic and intrinsic apoptosis pathways, and autophagy in tumor cells, among other mechanisms (8). Trichostatin A (TSA) vorinostat, entinostat and belinostat (Fig. 1) are some of the most known HDAC inhibitors (9).

Belinostat was approved by the Food and Drug Administration in 2014 for the treatment of peripheral

T-cell lymphoma (10). However, effectiveness of belinostat over BC has been also reported (11). Han *et al* (12) reported a significantly viability inhibition of the triple-negative BC (TNBC) MDA-MB-231 cells, suppressing its migration and invasion after belinostat treatment. On the other hand, Tuncer *et al* (13,14) demonstrated that belinostat inhibited the cell proliferation of MCF-7 cells with IC_{50} at μM range; meanwhile Lu *et al* (15) reported its effectiveness over *in vivo* breast tumors.

Coumarin, a 2H-chromen-2-one heterocycle, is a privileged scaffold with several medicinal properties (16). Coumarins have been reported to have a wide variety of pharmacological activities, among them, anticancer (17). A previous study reported the anticancer behavior of coumarins by different mechanisms including HDAC inhibition (18).

Following the authors' recent study on developing anticancer compounds targeting HDAC6 (19), in the present study, a set of six of 3-carboxy-coumarin sulfonamides, based in belinostat design, were synthesized. Docking studies were performed to obtain the free binding energies and to explore the interactions between the designed compounds and HDAC6. The synthesized compounds were evaluated for their cytotoxic activity against the BC cell lines MCF-7 and MDA-MB-231 and the nonmalignant cells 3T3/NIH.

Materials and methods

Materials and equipment. The progress of all the reactions was monitored by thin layer chromatography with ethyl acetate-hexane mixtures as eluent. Salicylaldehyde, diethyl malonate, ethyl benzoylacetate, piperidine, chlorosulfonic acid, aniline, benzylamine and phenethylamine were purchased from MilliporeSigma and used as received. The ACS grade solvents were purchased from CTR Scientific (https://ctrscientific.com/) and used without further purification. Melting points were measured on an Electrothermal Mel-Temp 1201D apparatus. IR spectra were collected using Varian 3100 FT-IR EXCALIBUR series spectrophotometer (Tecan Group, Ltd.). All NMR spectra were recorded in a Bruker advance TM-400 spectrometer (400 MHz ^{1}H NMR, 100 MHz ^{13}C NMR) in DMSO-d_6 or $CDCl_3$ solutions using $(CH_3)_4Si$ as an internal reference compound; chemical shifts (δ) are in ppm and coupling constants (^nJ H-H) in Hz.

General procedure for synthesis of coumarins 2, 6. Salicylaldehyde 1, diethyl malonate or ethyl benzoylacetate, and piperidine were dissolved in 15 ml of ethanol and placed under reflux at 78˚C for 24 h. After cooling, the solvent was removed by vacuum filtration, and the resulting solid was recrystallized from cold ethanol.

General procedure for synthesis of sulfonyl chlorides 3, 7. One g of 1 or 2 was placed in a 25 ml ball flask and 15 equivalents of chloro-sulfonic acid were added dropwise with stirring and cooling. Ice bath was removed, and the reaction mixture was heated at 115˚C for 2 h. The cooled solution was added dropwise to an ice-water mixture. The solid product was separated by vacuum filtration, washed with cold water and dried at room temperature.

General procedure for synthesis of sulfonamides 4, 5, 8a-c. One gram of 3 or 7 and 2.2 equivalents of triethylamine were dissolved in 20 ml of THF, dioxane or ethyl acetate, then 2.2 equivalents of the amines a-c were added dropwise with stirring at room temperature for 1 to 24 h. Sulfonamides were purified by open column chromatography using a silica gel 60 (0.063-0.200 mm) column (Merck KGaA), with dimensions of 3 cm in diameter and 50 cm in height. The mobile phase was passed through the column at a flow rate of 2 ml/min, using ethyl acetate-hexane mixtures as eluent. Spectroscopic data was presented in Table SI.

Ethyl 2-oxo-2H-chromen-3-carboxylate (2). White crystals, yield 72%, m.p. 88-90˚C. IR (cm^{-1}) *v* (C=O) 1760, *v* (C=O) 1672. ^{1}H-NMR ($CDCl_3$), δ (ppm): 8.53 (1H, s, H-4), 7.63 (1H, dd, ^3J=7.3 Hz, H-7) 7.62 (1H, d, ^3J=8.2 Hz, H-5), 7.35 (1H, d, ^3J=7.8, H-8), 7.34 (1H, dd, ^3J=7.6 Hz H-6), 4.40 (2H, q, ^3J=7.2 Hz, H-12), 1.35 (3H, t, ^3J=7.2 Hz, H-13). ^{13}C-NMR ($CDCl_3$), δ (ppm): 163.0 (C-11), 156.6 (C-2), 155.1 (C-9), 148.4 (C-4), 134.3 (C-7), 129.5 (C-5), 124.8 (C-6), 118.3 (C-10), 117.8 (C-3), 116.6 (C-8), 61.8 (C-12), 14.1 (C-13). E. A. $C_{12}H_{10}O_4$ (%) Found: C (66.27), H (4.76); Calculated: C (66.05), H (4.62).

6-(Chlorosulfonyl)-2-oxo-2H-chromen-3-carboxylic acid (3). White solid, yield 72%, m.p. 96-99˚C. IR (cm^{-1}) *v* (C=O) 1731, *v* (C=O) 1692, *v* (S=O) 1174. ^{1}H-NMR (DMSO-d_6): δ (ppm): 8.77 (1H, s, H-4), 8.13 (1H, d, ^4J=2.0 Hz, H-5), 7.91-7.88 (2H, m, H-7, H-8). ^{13}C-NMR (DMSO-d_6), δ (ppm): 164.3 (C-11), 157.2 (C-2), 155.0 (C-9), 148.5 (C-4), 143.4 (C-6), 131.8 (C-7), 127.4 (C-5), 119.1 (C-10), 117.6 (C-3), 116.7 (C-8). E. A. $C_{10}H_5ClO_6S.10H_20$ (%) Found: C (26.09), H (5.58); Calculated: C (41.61), H (1.75).

2-oxo-N-phenyl-6-(phenylsulfamoyl)-2H-chromen-3-carboxamide (4a). White solid, yield 20%, m.p. 233-235˚C. IR (cm^{-1}) *v* (N-H) 3200, *v* (C=O) 1703, *v* (C=O) 1662, *v* (S=O) 1150. ^{1}H-NMR (DMSO-d_6), δ (ppm): 8.93 (1H, s, H-4), 8.47 (1H, d, ^4J=2.3 Hz, H-5), 8.03 (1H, dd, ^3J=7.1 Hz, ^4J=2.3 Hz, H-7), 7.71 (1H, d, ^3J=7.1 Hz, H-8), 7.72-7.02 (10H, m, H-13-15, H-17-19). ^{13}C-NMR (DMSO-d_6), δ (ppm): 160.1 (C-11), 159.8 (C-2), 156.36 (C-9), 146.3 (C-4), 138.7 (C-12), 137.9 (C-6), 136.7 (C-16), 131.7 (C-7), 129.7, 129.5 (C-14, C-18), 129.6 (C-5), 124.9, 124.8 (C-15, C-19), 122.7 (C-3), 120.8, 120.3 (C-13, C-17), 119.0 (C-10), 118.1 (C-8). E. A. $C_{22}H_{16}N_2O_5S$ (%) Found: C (62.98), H (3.92), N (6.52); Calculated: C (62.85), H (3.84), N (6.66).

2-oxo-N-(2-phenylethyl)-6-[(2-phenylethyl)sulfamoyl]-2H-chromene-3-carboxamide (4c). White solid, yield 22%, m.p. 192-194˚C. IR (cm^{-1}) *v* (N-H) 3331, *v* (C=O) 1710, *v* (C=O) 1655, *v* (S=O) 1152. ^{1}H-NMR ($CDCl_3$), δ (ppm): 8.89 (1H, s, H-4), 8.73 (1H, t, NH), 8.1 (1H, d, ^4J=2.1 Hz, H-5), 8.01 (1H, dd, ^3J=7.6 Hz, ^4J=2.2 Hz, H-7), 7.47 (1H, d, ^3J=7.6 Hz, H-8), 7.37-7.08 (10H, m, H-15-17, H-21-23), 3.76 (2H, dd, ^3J=6.6 Hz, H-12), 3.31 (2H, dd, ^3J=6.5 Hz, H-18), 2.97 (2H, t, ^3J=7.2 Hz, H-13), 2.82 (2H, t, ^3J=6.7 Hz, H-19).^{13}C-NMR ($CDCl_3$), δ (ppm): 160.5 (C-11), 160.2 (C-2), 156.2 (C-9), 147.1 (C-4), 138.5 (C-14), 137.4 (C-6), 137.3 (C-20), 131.7 (C-7), 128.9, 128.7, 128.6, 128.5 (C-15-16, C-21-22), 128.8 (C-5), 128.7

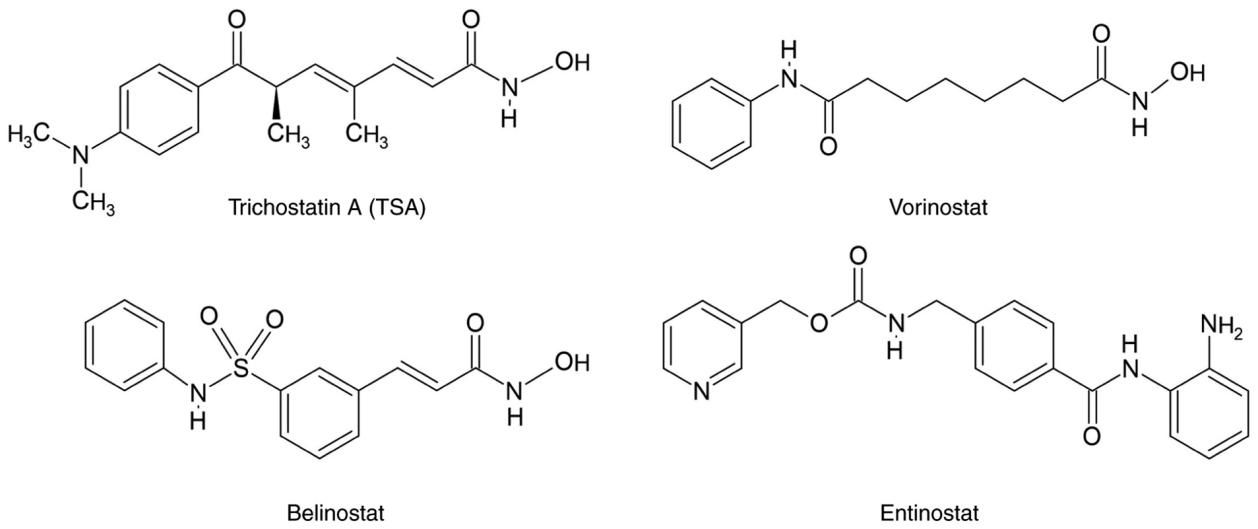

Figure 1. Structure of representative histone deacetylase inhibitors.

(C-17), 128.6 (C-23), 120.1 (C-3), 118.6 (C-10), 117.6 (C-8). E. A. $C_{26}H_{24}N_2O_5S$ (%) Found: C (66.03), H (5.36), N (5.83); Calculated: C (65.53), H (5.08), N (5.88).

N-benzyl-3-[(E)-(benzylimino)methyl]-4-hydroxybenzene-1-sulfonamide (5). Yellow crystals, yield 52%, m.p. 156-158˚C. IR (cm^{-1}) *v* (N-H) 3248, *v* (C=N) 1628, *v* (S=O) 1153. ^{1}H-NMR ($CDCl_3$), δ (ppm): 8.39 (1H, s, H-4), 7.80 (1H, d, ^4J=2.4 Hz, H-5), 7.77 (1H, dd, ^3J=8.8 Hz, ^4J=2.4 Hz, H-7) 7.42-7.20 (10H, m, H-13-15, H-18-20) 7.04 (1H, d, ^3J=8.8 Hz, H-8), 4.83 (2H, s, H-11) 4.14 (2H, d, ^3J=6.2 Hz, H-16).^{13}C-NMR ($CDCl_3$), δ (ppm): 166.2 (C-9), 164.5 (C-4), 136.9 (C-17), 136.2 (C-12), 134.9 (C-6), 131.6 (C-5), 131.1 (C-7), 129.3, 128.9, 128.7, 128.0, 127.9, 127.8 (C-13-15, C-18-20), 118.5 (C-8), 117.9 (C-16). E. A. $C_{21}H_{20}N_2O_3S$ (%) Found: C (66.56), H (5.68), N (7.22); Calculated: C (66.29), H (5.29), N (7.36).

3-Benzoyl-2H-chromen-2-one (6). White crystals, yield 71%, m.p. 134-136˚C. IR (cm^{-1}) *v* (C=O) 1717, *v* (C=O) 1656. ^{1}H-NMR ($CDCl_3$), δ (ppm): 8.11 (1H, s, H-4), 7.91 (2H, dd, ^3J=7.1, ^4J=1.6 Hz, H-13), 7.70-7.64 (2H, m, H-7, H-15), 7.63 (1H, d, ^3J=7.6 H-5), 7.51 (2H, dd, ^3J=7.8 Hz, H-14), 7.44 (1H, d, ^3J=8.3 H-8), 7.38 (1H, dd, ^3J=7.4, H-6). ^{13}C-NMR ($CDCl_3$), δ (ppm): 191.6 (C-11), 158.3 (C-2), 154.8 (C-9), 145.3 (C-4), 136.2 (C-12), 133.8 (C-5), 133.6 (C-15), 129.5 (C-13), 129.1 (C-7), 128.6 (C-14), 127.1 (C-3), 124.9 (C-6), 118.2 (C-10), 116.9 (C-8). E. A. $C_{16}H_{10}O_3$ (%) Found: C (76.43), H (4.11); Calculated: C (76.79), H (4.03).

3-[3-(Chlorosulfonyl)benzoyl]-2-oxo-2H-chromen-6-sulfonyl chloride (7). White solid, yield 85%, m.p. 75-78˚C. IR (cm^{-1}) *v* (C=O) 1743, *v* (C=O) 1665, *v* (S=O) 1167. ^{1}H-NMR (DMSO-d_6), δ (ppm): 8.53 (1H, s, H-4), 8.10 (1H, d, ^4J=2.0 Hz, H-5), 8.08 (1H, dd, ^4J=1.6 Hz, H-13), 7.92 (1H, dd, ^3J=8.0 Hz, ^4J=2.0 Hz, H-15), 7.90 (2H, dd, ^3J=7.7 Hz, ^4J=1.6 Hz, H-7, H-15), 7.52 (1H, dd, ^3J=7.8 Hz, H-16), 7.46 (1H, d, ^3J=8.6 Hz, H-8). ^{13}C-NMR (DMSO-d_6), δ (ppm): 191.1 (C-11), 158.4 (C-2), 154.4 (C-9), 149.0 (C-14), 146.0 (C-4), 145.4 (C-6), 136.1 (C-12), 131.4 (C-17), 131.2 (C15), 130.7 (C-7), 128.9 (C-16), 127.1 (C-13), 126.8 (C-3), 126.1 (C-5), 117.8 (C-10), 116.4 (C-8). E. A. $C_{16}H_8Cl_2O_7S_2$. $10H_2O$ (%) Found: C (30.68), H (4.58); Calculated: C (42.97), H (1.80).

2-oxo-N-phenyl-3-[3-(phenylsulfamoyl)benzoyl]-2H-chromene-6-sulfonamide (8a). Brown solid, yield 25%, m.p. 94-96˚C. IR (cm^{-1}) *v* (N-H) 3237, *v* (C=O) 1723, *v* (C=O) 1669, *v* (S=O) 1151. ^{1}H-NMR (DMSO-d_6), δ (ppm): 8.54 (1H, s H-4), 8.33 (1H, d, ^4J=2.3 Hz, H-5), 8.22 (1H, dd, ^4J=1.6 Hz, H-13), 8.17 (1H, dd, ^3J=7.8 Hz, ^4J=1.6 Hz, H-17), 8.05 (1H, dd, ^3J=7.3 Hz, ^4J=2.3 Hz, H-7), 8.01 (1H, dd, ^3J=7.8 Hz, ^4J=1.7 Hz, H-15), 7.69 (1H, dd, ^3J=7.8 Hz, H-16), 7.68 (1H, d, ^3J=7.3 Hz, H-8), 7.26-7.0 (10H, m, H-19-21, H-23-25). ^{13}C-NMR (DMSO-d_6), δ (ppm): 190.6 (C-11), 157.7 (C-2), 156.9 (C-9), 145.8 (C-4), 140.8 (C-12), 137.6, 137.6 (C-18, C-22), 137.0 (C-6), 136.4 (C-14), 134.2 (C-17), 131.8, 131.7 (C-7, C-15), 130.5 (C-16), 129.8, 129.7 (C-20, C-24), 129.4 (C-5),127.4 (C-13), 127.3 (C-3), 125.0, 124.9 (C-21, C-25), 121.1, 120.8 (C-19, C-23), 118.9 (C-10), 118.3 (C-8). E. A. $C_{28}H_{20}N_2O_7S_2$ (%) Found: C (60.14), H (3.93), N (5.11); Calculated: C (59.99), H (3.59), N (4.99).

N-benzyl-3-[3-(benzylsulfamoyl)benzoyl]-2-oxo-2H-chromene-6-sulfonamide (8b). White crystals, yield 42%, m.p. 168-170˚C. IR (cm^{-1}) *v* (N-H) 3305, *v* (C=O) 1722, *v* (C=O) 1676, *v* (S=O) 1153. ^{1}H-NMR (DMSO-d_6), δ (ppm): 8.98 (1H, s H-4), 8.85 (1H, dd, ^4J=1.7 Hz, H-13), 8.79 (1H, d, ^4J=2.2 Hz, H-5), 8.69 (1H, dd, ^3J=7.8 Hz, ^4J=2.3 Hz, H-17), 8.62-8.60 (2H, m, H-7, H-15), 8.22 (1H, dd, ^3J=7.8 Hz, H-16), 8.05 (1H, d, ^3J=8.7 Hz, H-8), 7.74-7.68 (10H, m, H-20-22, H-25-27), 4.66 (4H, d, ^3J=6.0 Hz, H-18, H-23). ^{13}C-NMR (DMSO-d_6), δ (ppm): 190.5 (C-11), 157.7 (C-2), 157.2 (C-9), 145.5 (C-4), 142.5 (C-12), 138.4 (C-6), 137.7, 137.7 (C-19, C-24), 136.6 (C-14), 133.4 (C-17), 132.0, 132.0 (C-7, C-15), 130.1 (C-16), 129.5 (C-5), 128.8, 128.4, 128.3, 127.9, 127.8 (C-20-22, C-25-27), 128.0 (C-3), 127.8 (C-13), 118.9 (C-10), 118.0 (C-8), 47.3 (C-18, C-23). E. A. $C_{30}H_{24}N_2O_7S_2$ (%) Found: C (61.58), H (4.29), N (4.85); Calculated: C (61.21), H (4.11), N (4.76).

2-oxo-N-(2-phenylethyl)-3-{3-[(2-phenylethyl)sulfamoyl] benzoyl}-2H-chromene-6-sulfonamide (8c). Brown solid, yield 22%, m.p. 78-80˚C. IR (cm^{-1}) *v* (N-H) 3274, *v* (C=O) 1724, *v* (C=O) 1667, *v* (S=O) 1148. ^{1}H-NMR (DMSO-d_6): δ (ppm): 8.98 (1H, s H-4), 8.85 (1H, s, H-13), 8.78 (1H, d, ^{4}J=1.9 Hz, H-5), 8.68 (1H, dd, ^{3}J=7.8 Hz, ^{4}J=1.6 Hz, H-17), 8.60 (2H, dd, ^{3}J=7.4 Hz, ^{4}J=2.0 Hz, H-7, H-15), 8.21 (1H, dd, ^{3}J=7.8 Hz, H-16), 8.05 (1H, d, ^{3}J=7.4 Hz, H-8), 7.70-7.61 (10H, m, H-21-23, H-27-29), 3.73-3.65 (4H, m, H-18, H-24) 3.29-3.24 (4H, m, H-19, H-25). ^{13}C-NMR (DMSO-d_6), δ (ppm): 190.6 (C-11), 157.9 (C-2), 157.3 (C-9), 145.9 (C-4), 142.3 (C-12), 139.1, 139.0 (C-20, C-26), 138.1 (C-6), 137.7 (C-14), 133.5 (C-17), 131.9, 131.9 (C-7, C-15), 130.2 (C-16), 129.4 (C-5), 129.2, 129.2, 128.8, 126.8 (C-21-23, C-27-29), 128.0 (C-3), 127.7 (C-13), 119.1 (C-10), 118.0 (C-8), 45.0, 44.9 (C-18, C-24), 36.2 (C-19, C-25). E. A. $C_{32}H_{28}N_2O_7S_2$ (%) Found: C (62.78), H (4.94), N (4.62); Calculated: C (62.32), H (4.58), N (4.54).

Molecular docking. Molecular docking was performed using the AutoDock Vina tool implemented in UCSF Chimera version 1.16 (www.cgl.ucsf.edu/chimera). 3D structures of the test compounds were constructed using Maestro version 13.3 (Schrodinger, Inc.). The protein structure of HDAC was retrieved from the Protein Data Bank (https://www.rcsb.org/) with the accession code 5EDU. All water molecules and also the co-crystallized ligands were removed from the crystallographic structure. The grid box was defined surrounding the co-crystallized ligand trichostatin A (TSA) within the HDAC6 active site. The grid box size was set at 20 Å, 20 Å, and 20 Å (x, y and z). In all simulations, the ligands were flexible, and the protein remained static. 2D protein-ligand interaction diagrams were generated through Maestro. Validation was performed using AutoDock Vina tool in UCSF Chimera 1.16 by redocking the co-crystallized ligand TSA. The 3D structure of TSA was built through Maestro 13.3 and docked within the active site of HDAC6 (5EDU). The grid box was centered at the crystallographic coordinates of the co-crystallized ligand, and the grid box size was set at 20 Å, 20 Å, and 20 Å. This validation was carried out based on important interactions.

In vitro assays

Cell culture. A total of three cell lines were used to evaluate the synthesized compounds: The human TNBC cell line MDA-MB-231 (cat. no. HTB-26), the human BC cell line MCF-7 (cat. no. HTB-22) and the NIH/3T3 mouse fibroblast cell line. MCF-7 and MDA-MB-231 BC cell lines were obtained from the American Type Culture Collection. The MDA-MB-231 and MCF-7 BC cell lines were selected for the present study due to their well-documented characteristics. MDA-MB-231 is a TNBC cell line known for its aggressive and invasive properties, representing a challenging subtype of BC. By contrast, MCF-7 is an estrogen receptor-positive cell line that is less aggressive and more responsive to hormone therapy.

The NIH/3T3 cell line was obtained from the Parasitology Laboratory, Faculty of Medicine, Public Health, and Nursing (FKKMK), University Gadjah Mada (Sleman, Indonesia). This cell line is widely used to assess cellular mechanisms and was chosen to provide a baseline for comparing the effects of the synthesized compounds. Given that HDAC6 inhibition has been shown to reverse metastatic traits and restore normal cellular organization in cancer cells, NIH/3T3 cells, which do not exhibit these malignancy-associated traits, offer a valuable control. NIH/3T3 cells were included as non-malignant controls. All of them were cultured in Dulbecco's modified Eagle's Medium (DMEM) supplemented with 10% fetal bovine serum (FBS, Biowest; https://biowest.net/) and 1% antibiotic-antifungal (penicillin G, sodium salt and 1% streptomycin sulfate). Cell cultures were incubated at 37˚C under a 5% CO_2 and 95% air atmosphere; PBS-Trypsin-EDTA solution was used to detach the cells when their confluency was up to 80%, and cells were seeded in a 96-plate well with $10x10^3$ cells in each well. After 24 h, the medium was replaced by compounds at concentrations of 6.25, 12.5, 25, 50 and 100 μM, previously dissolved in DMSO (0.1%). For manipulation and visualization, a biosafety level 2 vertical laminar flow cabinet (NUAIRE A2 NU-543-400) and an inverted binocular microscope (MOTIC AE-20) were used, respectively.

Viability assay. Cells were seeded in a tissue culture (TC)-treated 96-well flat-bottom microplate (Corning, Inc.) at a density of $1x10^4$ cells/well in supplemented DMEM-HG and incubated for 24 h. Afterward, the medium was removed, replaced with the treatments previous described in a final volume of 100 μl/well, and the cells were incubated for 48 h in a 5% CO_2 atmosphere at 37˚C. At the end, the treatments were removed and replaced with 100 μl/well 1X Alamar Blue™ Cell Viability Assay Reagent (MilliporeSigma) in phenol red-free medium for 4 h. The optical density was measured on a microplate reader (iMark; Bio-Rad Laboratories, Inc.) at a wavelength of 570-600 nm for excitation-emission. The percentage of cytotoxicity was calculated as: 100-[(experimental OD value-blank OD value)/(control OD value-blank OD value) x100%]. Cisplatin (58.32 μM), doxorrubicin (2 μM) and belinostat (40 μM) (MilliporeSigma) were used as positive controls. The compounds 4a, c, 5, and8a-c were evaluated at a concentration of 40 μM.

Isolation of lymphocytes from human peripheral blood and cell viability test. The methodology for isolation of lymphocytes from human peripheral blood and cell viability test was performed according to the methodology of Calderón-Segura *et al* (20) and Hernández-Fuentes *et al* (21) with slight modifications. A total of 20 ml of heparinized venous blood from three healthy volunteer donors was centrifuged at 500 x g for 20 min at room temperature (22-25˚C). The resulting cellular layer was diluted 1:1 with HBSS, layered over Ficoll-Paque, and centrifuged at 250 x g for 10 min at room temperature (22-25˚C). Lymphocytes were then collected, washed twice in RPMI-1640 medium (Biowest, Inc.) by centrifugation at 250 x g at room temperature (22-25˚C) for 10 min, and resuspended in RPMI-1640 medium (37˚C) supplemented with 1% penicillin/streptomycin. The lymphocyte pellet was immediately assessed for cellular viability using a Neubauer chamber. Cell viability was determined before and after treatments using the trypan blue exclusion method, where trypan blue penetrates the damaged membrane of dead cells and stains the nucleus. A mixture of 10 μl of cell pellet and 10 μl of trypan blue was incubated for 3 min, and then the number of dead cells out of 100 consecutive cells was counted in duplicate (20,21). The compounds (4a, c, 5, 8a-c) and belinostat were evaluated at a concentration of 40 μM.

All experiments were performed in triplicate in independent assays.

The present study was approved by the Ethics Committee of the Clinical Research Center of the National Cancer Institute (approval no. CEICANCL23062023-DISULFA-21; Colima, Mexico). Cells were isolated from three healthy male volunteer donors, all of whom provided oral informed consent for the collection of their samples. The donors were aged between 26-27 years, with no history of drug use or medication intake 72 h prior to the sample collection.

Statistical analysis. The results are presented as the mean ± standard deviations (SD). In the *viability assay*, the data represent the mean of three independent experiments with 10 replicates per experiment. Group differences were evaluated using the Kruskal-Wallis statistical test, followed by a Dunn's post hoc test for multiple comparisons. All statistical analyses were conducted using SPSS Statistics 20 software (IBM Corp.). Statistically significant difference is denoted by the corresponding symbols in the figures for $P<0.05$, were necessary.

Results and Discussion

Design features of 3-carboxy-coumarin sulfonamides. The general pharmacophore model for the HDAC inhibitors essentially consists in three parts: i) A cap group, a hydrophobic region that interacts with the external domain of the enzyme; ii) a zinc binding group (ZBG) that coordinates the zinc ion in the active site of the enzyme; and iii) a linker, a semi-flexible chain (generally a six carbon unsaturated chain) that connects the cap group and the ZBG and set them in within the binding site for interactions (22-24).

Hydroxamate is the most common ZBG for its strong binding affinity with metal ions; however, this feature leads to lack of selectivity, binding to multiple metalloenzymes, generating side effects, besides being metabolically unstable (25,26). Additionally, numerous other studies have reported non-hydroxamate inhibitors with significant *in vitro* activity over HDACs (27-29). On the other hand, numerous studies indicated that HDAC6 active site cavity is wider and shallower than other isoforms, allowing to accommodate bulkier molecules (30-32). Moreover, aromatic moieties are useful for increasing affinity and selectivity for HDAC6 (33,34). In this context, the coumarin scaffold was incorporated on the linker region (Fig. 2), maintaining the sulfonamide moiety, the aromatic central ring and the α,β-unsaturated system of belinostat; and the hydroxamate moiety was replaced by the same aromatic substituents used in the cap group.

Chemistry. The synthesis of the designed sulfonamides 4a, c, 5 and 8a-c is demonstrated in Fig. 3. This approach includes a three-step reaction sequence. Coumarins (2,6) were synthesized by the Knoevenagel condensation of salicylaldehyde with the corresponding ketone in accordance with previously described methods (35,36). Chlorosulfonation of 2 and 6 was carried out without solvent, with a large excess of chlorosulfonic acid and under reflux to provide sulfonyl chlorides 3 and 7 in favorable yields. The treatment of sulfonyl chloride 3 with aniline or/and phenethylamine provided sulfonamides

Table I. Selected chemical shifts in ppm (^{1}H-NMR/^{13}C-NMR) for compounds 2-8c in $CDCl_3$ or DMSO-d_6 at 400 MHz.

Compound	H-4	C-6	NH_A	NH_B
2[a]	8.53	124.8	-	
6[a]	8.11	124.9		
3[b]	8.77	143.4		
7[b]	8.53	145.4		
4a[b]	8.93	137.9	10.68	10.54
4c[a]	8.89	137.4	4.60	8.73
5[a]	-	134.9	4.83	-
8a[b]	8.54	137.0	10.52	10.40
8b[b]	8.98	138.4	7.62	7.62
8c[b]	8.98	138.1	7.23	7.28

[a]$CDCl_3$; [b]DMSO-d_6.

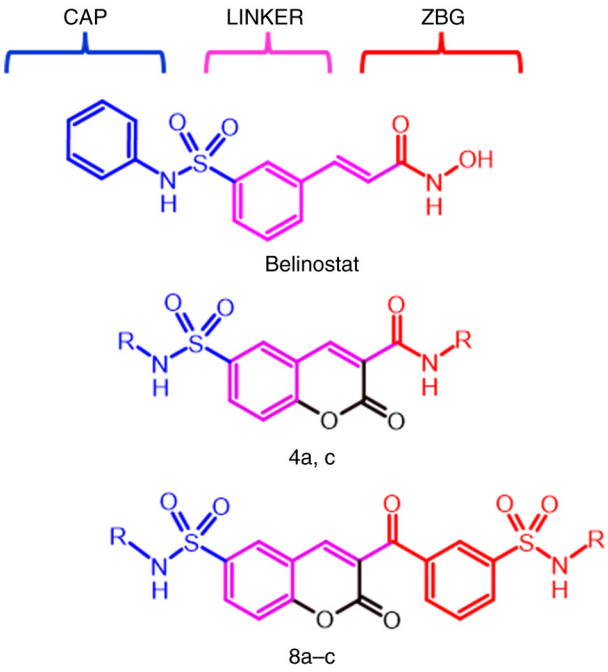

Figure 2. Design of 3-carboxy-coumarin sulfonamides (compounds 4a, 5, 8b, 8c, 4c and 8a).

4a, c meanwhile with benzylamine provided 5 probably due to steric effects. On the other hand, treatment of 7 with the corresponding amines provided sulfonamides 8a-c. All sulfonamides were obtained at room temperature in the presence of triethylamine as a base.

In the ^{1}H NMR spectra the H-4 signal indicated the formation of coumarins (2,6), observed as the most de-shielded signal due to the intramolecular hydrogen bond with the O-carbonyl as previously reported by García-Báez *et al* (37). H-4 appeared in 8.53 ppm in compound 2 and shifted to higher frequencies in the 8.89-8.93 ppm range due to amide formation in 4a, c; meanwhile it shifted from 8.11 ppm in compound 6 to 8.54-8.98 ppm in sulfonamides 8a-c (Table I). The chemical shifts of sulfonamide N-H proton

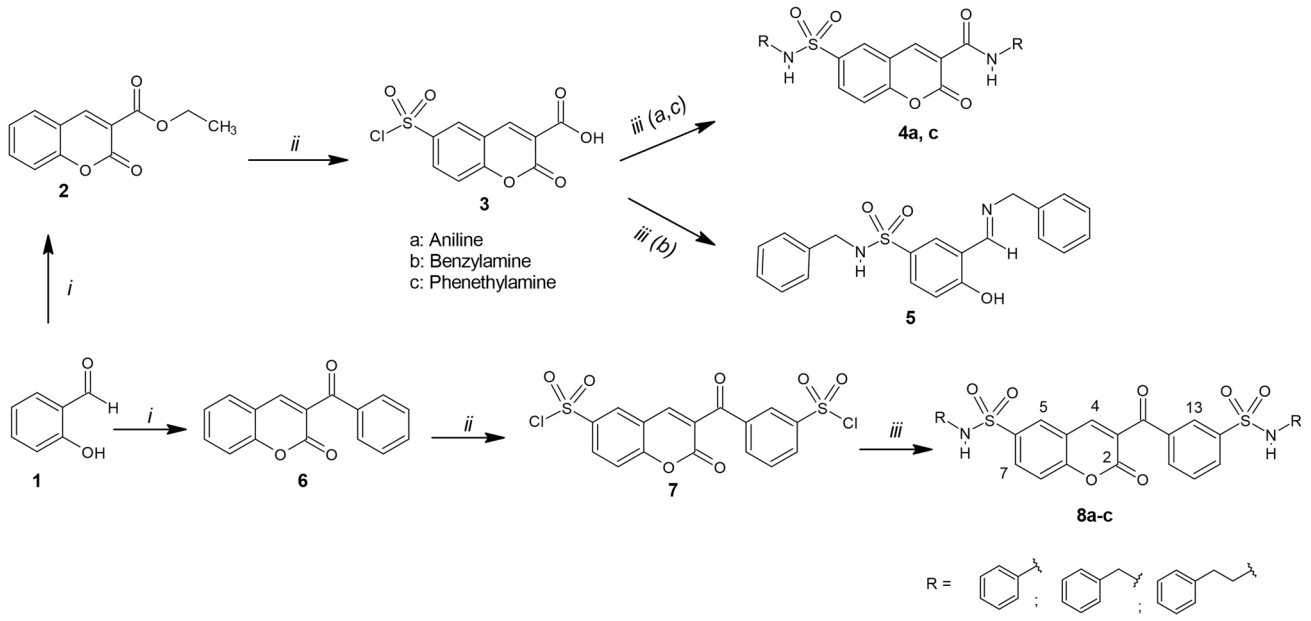

Figure 3. Scheme of synthesis of 3-carboxy-coumarin sulfonamides 4a, c, 5 and 8a-c. Reagents and conditions: i) Diethyl malonate/ethyl benzoylacetate, piperidine, EtOH, reflux 24 h; ii) HSO_3Cl, reflux 2 h; iii) amines (a, b, c), Et_3N, THF, stirring 1-24 h, room temperature.

varied according to the amine residue; the N-H signals were observed in the 4.60-7.62 ppm range with the alkylamines benzylamine and phenylethylamine (compounds 4c, 5, 8b-c), whereas with aniline (compounds 4a, 8a) the N-H appeared in the 10.40-10.68 ppm range. The amidic N-H proton appeared in 8.73-10.54 ppm range in compounds 4a, c. The aromatic protons appeared as expected in the region 7.34-7.63 ppm for 2 and 6, 7.52-8.13 ppm for 3 and 7, and 7.69-8.79 ppm for 4a-8c (Table SI).

The ^{13}C NMR spectra C-6 carbon was de-shielded from 124.8-124.9 ppm range in compounds 2 and 7 to 143.4-145.4 ppm range in compounds 3 and 7 after chlorosulfonation reaction occurred; meanwhile in the sulfonamides 4a, c, 5, 8a-c it was observed in the 134.9-138.4 ppm range due to the electron-donor effect of the amines. The IR spectra (Figs. S1 and S2) showed four characteristic stretching absorption bands at 3331-3200, 1760-1703, 1692-1656 and 1174-1151 cm^{-1} corresponding to sulfonamide N-H, exocyclic C=O, lactonic C=O and S=O, respectively.

Molecular docking. To determine the possible interaction mode between the synthesized compounds (4a, c, 5 and 8a-c) and the HDAC6 catalytic site, molecular docking was performed using a validated molecular program (Chimera 1.16). Validation of the method was performed by redocking the co-crystallized ligand TSA where coordination with zinc ion of HDAC6 in a bidentate fashion was observed (Fig. S3). The molecular docking studies showed that all ligands reached the catalytic binding site of HDAC6.

Free binding energies ΔG (kcal/mol) are listed in Table II. ΔG values are in the -6.9 to -8.7 kcal/mol range, close to the value obtained for the reference compound, belinostat (-8.3 kcal/mol). Compounds 8a-c, having an additional aromatic ring, exhibit the most favorable ΔG values, being close or even higher than belinostat in some cases. This is consistent with previous studies suggesting that the HDAC6 catalytic cavity is wider than other isoforms, thus bulky aromatic rings are well tolerated in the molecule design (38).

All ligands interact with Ser 568, Phe 620, Hid 651, Phe 679 and Phe 680 amino acid residues (Fig. 4), which are common interactions among the HDAC6 inhibitors (39-42). These interactions are similar to those found in belinostat (Gly 619, Hid 651, Phe 679 and Phe 680) where the main difference is that in ligands 4a, c, 5, 8a-c no coordination with the zinc ion is observed which can be explained by the absence of a traditional ZBG as N-OH in these ligands. As can be observed, hydrogen bonding is formed between sulfonamide N-H of compound 8a and Ser568; meanwhile, the N-R-phenyl moiety of all ligands is involved in π-π interactions with the aromatic residues surrounding the HDAC6 cavity.

In vitro evaluation. In a preliminary study, the cytotoxic efficacy of six newly synthesized compounds was evaluated in the MDA-MB-231 cell line, alongside three control agents-belinostat, cisplatin and doxorubicin. The compounds, which share structural similarities with belinostat, were tested to determine their comparative effectiveness. Belinostat, tested at a concentration of 40 μM, served as a direct comparator given its structural relevance. The well-established chemotherapy agents, cisplatin at 58.32 μM and doxorubicin at 2 μM, known for their potent cytotoxic effects in this cell line, served as benchmarks. The evaluation included compounds labeled as 4a, 5, 8b, 8c, 4c and 8a.

The results, shown in Fig. 5, highlight the cytotoxic activities (expressed as percentages) of the compounds tested. Compounds 4a, 5, 8c, 4c and 8a exhibited lower cytotoxic activity levels, though comparable to that of doxorubicin. It is important to emphasize that, although the mean inhibition percentages were slightly lower, only compounds 4 and 4c showed statistically significant differences when compared individually to doxorubicin ($P<0.05$, for both comparisons). The other compounds (5, 8b, 8c and 8a) did

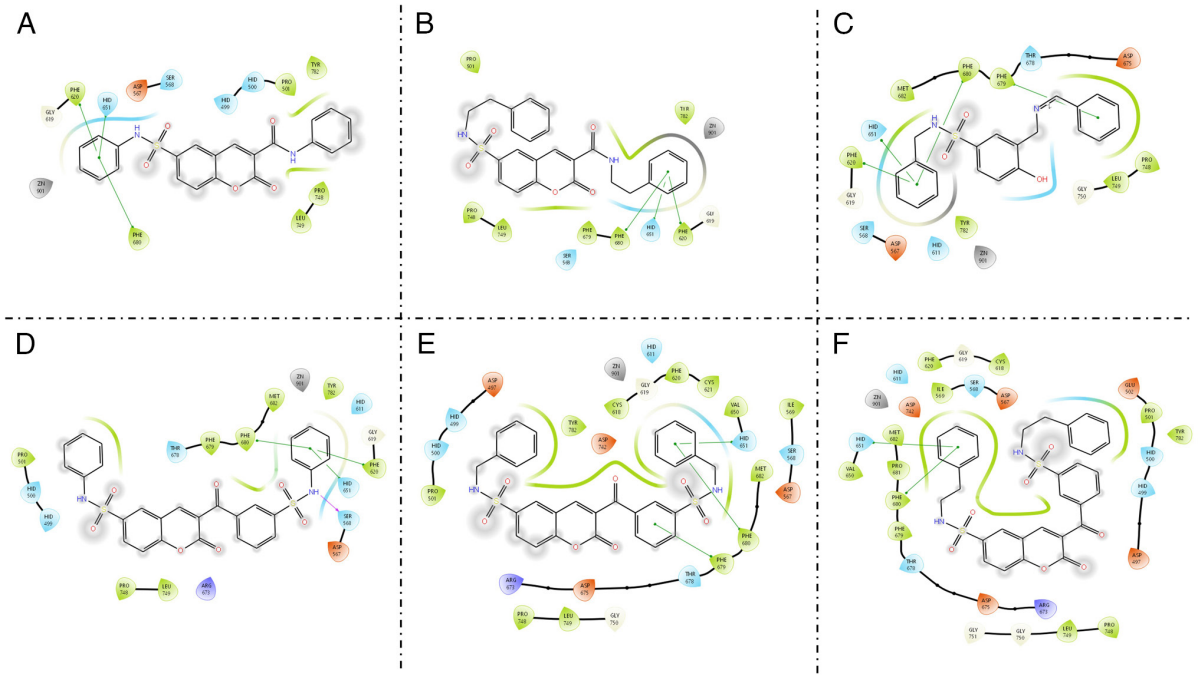

Figure 4. 2D representation of the interactions of compounds (A) 4a, (B) 4c, (C) 5, (D) 8a, (E) 8b and (F) 8c with the HDAC6 catalytic site. Pink color represents the hydrogen bond interaction and green color represents the π-π interaction.

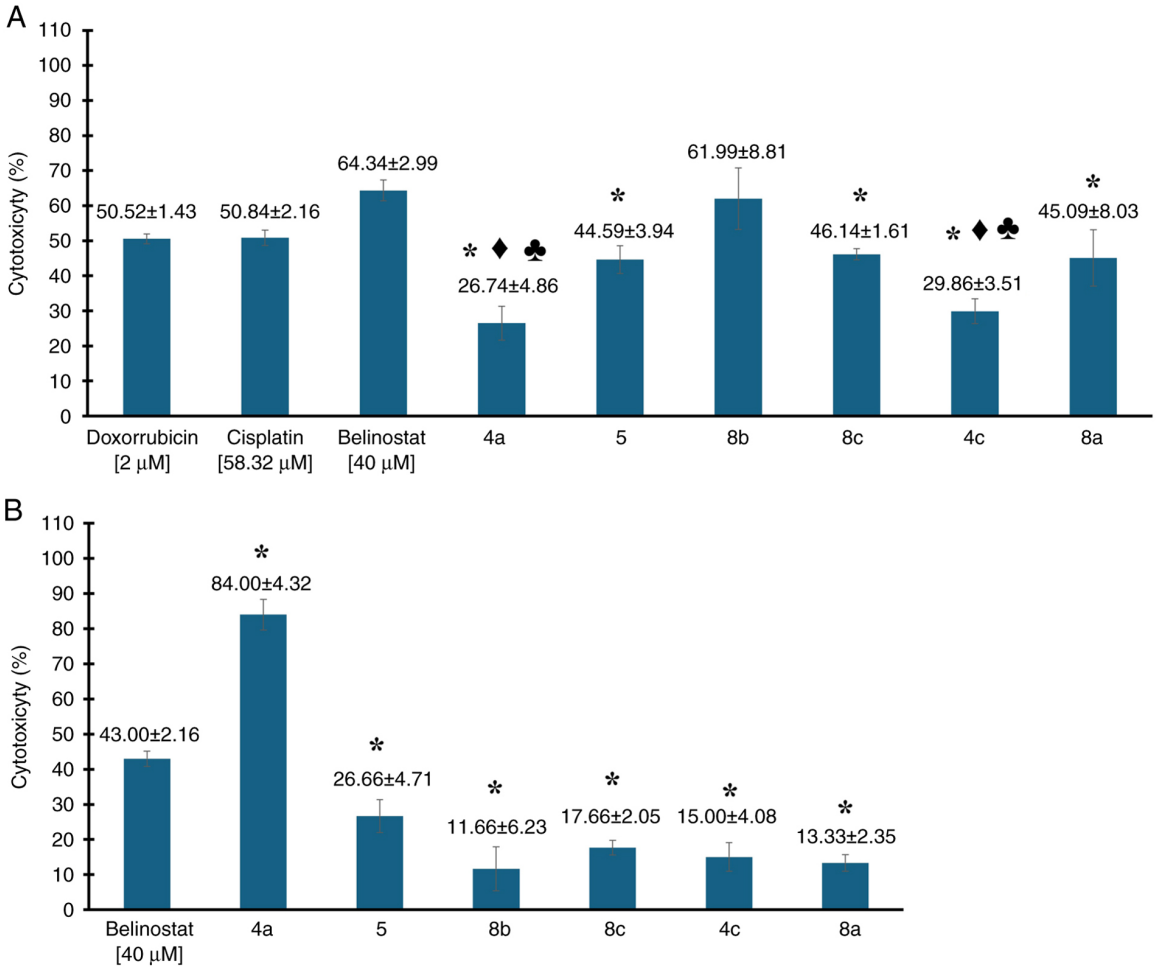

Figure 5. (A) Preliminary evaluation of cytotoxic activity of 3-carboxy-coumarin sulfonamides (compounds 4a, 5, 8b, 8c, 4c and 8a) at 40 μM in MDA-MB-231 cell line, compared with standard chemotherapeutic agents belinostat (40 μM), doxorubicin (2 μM) and cisplatin (58.32 μM). (B) Evaluation of leukocyte viability after exposure to compounds 4a, 5, 8b, 8c, 4c and 8a and belinostat at 40 μM. Data are presented as the mean ± SD. All assays were performed in triplicate. *P<0.05 vs. belinostat; ♦P<0.05 vs. doxorrubicin; ♣P<0.05 vs. cisplatin.

Table II. Binding energies ΔG (kcal/mol) of molecules docked into the active site of histone deacetylase 6.

Compounds	ΔG (Kcal/mol)
4a	-7.4
4c	-6.9
5	-7.2
8a	-8.7
8b	-8.3
8c	-7.9
Belinostat	-8.3

Table III. IC_{50} values of compounds 5, 8b and 8c.

Compound	MCF-7	MDA-MB-231	NIH/3T3
5	71±8 μM	85±12 μM	60±5 μM
8b	25±4 μM	17±2 μM	46±3 μM
8c	30±2 μM	39±6 μM	73±6 μM

These IC_{50} values represent the concentrations of each compound required to inhibit 50% of cell proliferation under the experimental conditions used. The data are expressed as the mean ± standard deviation, indicating the cytotoxic potency of each compound in inhibiting cell proliferation in both human breast cancer cell lines (MCF-7 and MDA-MB-231) and a mouse fibroblast cell line (NIH/3T3). Results for at least three independent experiments.

not present statistically significant differences (P>0.05, for all comparisons) under the conditions of the analysis performed. Regarding cisplatin, another chemotherapeutic agent used to treat this type of cancer, a similar trend was observed to that with doxorubicin. Compounds 4a, 5, 8c, 4c and 8a exhibited lower cytotoxic activity levels compared with cisplatin. However, only compounds 4 and 4c showed statistically significant differences when individually compared with cisplatin (P<0.05, for both comparisons). The other compounds (5, 8b, 8c and 8a) did not present statistically significant differences (P>0.05, for all comparisons) under the conditions of the analysis performed. Notably, compound 8b exhibited a 1.12-fold greater potency than cisplatin at comparable concentrations, demonstrating the highest cytotoxic activity with an average of 61.99±8.82%. This was followed by compound 8c, which showed 46.14±1.61% cytotoxicity, and compound 8a, with 45.09±8.03%. These results highlight 8b, 8a and 8c as the most potent compounds, prompting further detailed cytotoxicity testing in the MDA-MB-231 cell lines.

On the other hand, under the tested conditions, belinostat exhibited cytotoxic activity at 64.34±2.99%. Although belinostat is primarily used to treat other cancers, such as peripheral T-cell lymphoma, it serves as the core structure for the compounds examined. However, in preliminary evaluations, compounds 4a, 5, 8c, 4c and 8a exhibited lower cytotoxicity percentages compared with belinostat. Notably, compound 8b showed inhibition percentages similar to those of belinostat, without statistically significant differences (P=0.459). By contrast, the rest of the compounds demonstrated statistically significant differences when compared with belinostat (P<0.05, for all comparisons). Additionally, morphological changes were observed in MCF-7, MDA-MB-231 and NIH/3T3 cells incubated with different concentrations of compounds 8c, 8b, and 5 (Figs. 6-8, respectively). These changes potentially alter the cell structure to a more spheroidal form, possibly affecting the cytoskeleton and related proteins. However, further studies are required to confirm these observations.

A brief structure-activity relationship analysis revealed some structural differences that could potentially account for the observed effects. For instance, compound 4a, which is structurally similar to belinostat, demonstrated a cytotoxic activity of 26.5%. This compound has a high structural analogy to belinostat but features a coumarin system replacing the aromatic ring (linker, Fig. 2) adjacent to the sulfonamide group. At this point it is important to highlight the fact that the sulfonamide group was proposed to be important to maintain the activity of the molecules; this last point correlates with the results obtained in the present study (24). Additionally, this the incorporation of a coumarin heterocycle has also been reported to increase the cytotoxicity activity against cancer cell lines such as MDA-MB-231 (43).

Compounds 5, 8a and 8c demonstrated cytotoxic activities exceeding 50% at a concentration of 40 μM. Dose-response curves were obtained to determine the IC_{50} values of compounds 5 and 8b-c against MCF-7, MDA-MB-231 and 3T3/NIH cells. All three compounds exhibited IC_{50} values in the micromolar range (17-85 μM, Table III). Compound 8b showed the best antiproliferative activity over both MCF-7 and MDA-MB-231 cell lines. However, compound 8c exhibited an improved safety profile, being less cytotoxic to normal 3T3/NIH cells and with similar IC_{50} values over MCF-7 and MDA-MB-231 to those of compound 8b.

It is important to note that there are slight structural differences among these compounds that could explain their effects. Specifically, compounds 8a-c all incorporate a coumarinic system within their structure. However, variations exist in the spacers (methylene groups, CH_2) between the aromatic ring and the sulfonamide-coumarin system. Compound 8a lacks methylene spacer, while compound 8b contains one methylene, and compound 8c has two methylene spacers. These structural variations result in cytotoxicity percentages of 45%, 62%, and 46%, respectively, as represented in Fig. 5A. These findings suggested that the presence and number of methylene spacers are critical factors influencing the cytotoxic activity of these compounds. This is a significant point for discussion in future research efforts to further elucidate the mechanism of action and optimize the therapeutic potential of these compounds.

Regarding compound 5, it structurally differs from the others previously discussed as it lacks the coumarinic system; however, it still exhibits a comparable level of cytotoxicity at 44%. A detailed analysis of its structure revealed a similarity to belinostat, with a critical distinction: Compound 5 incorporates a single methylene spacer between the aromatic ring and the sulfonyl group. This observation is noteworthy because, as observed with compounds 8a-c, the presence and number of methylene spacers have had a substantial impact on cytotoxic activity. These facts have been observed in other derivatives of compounds with HDAC activity, such

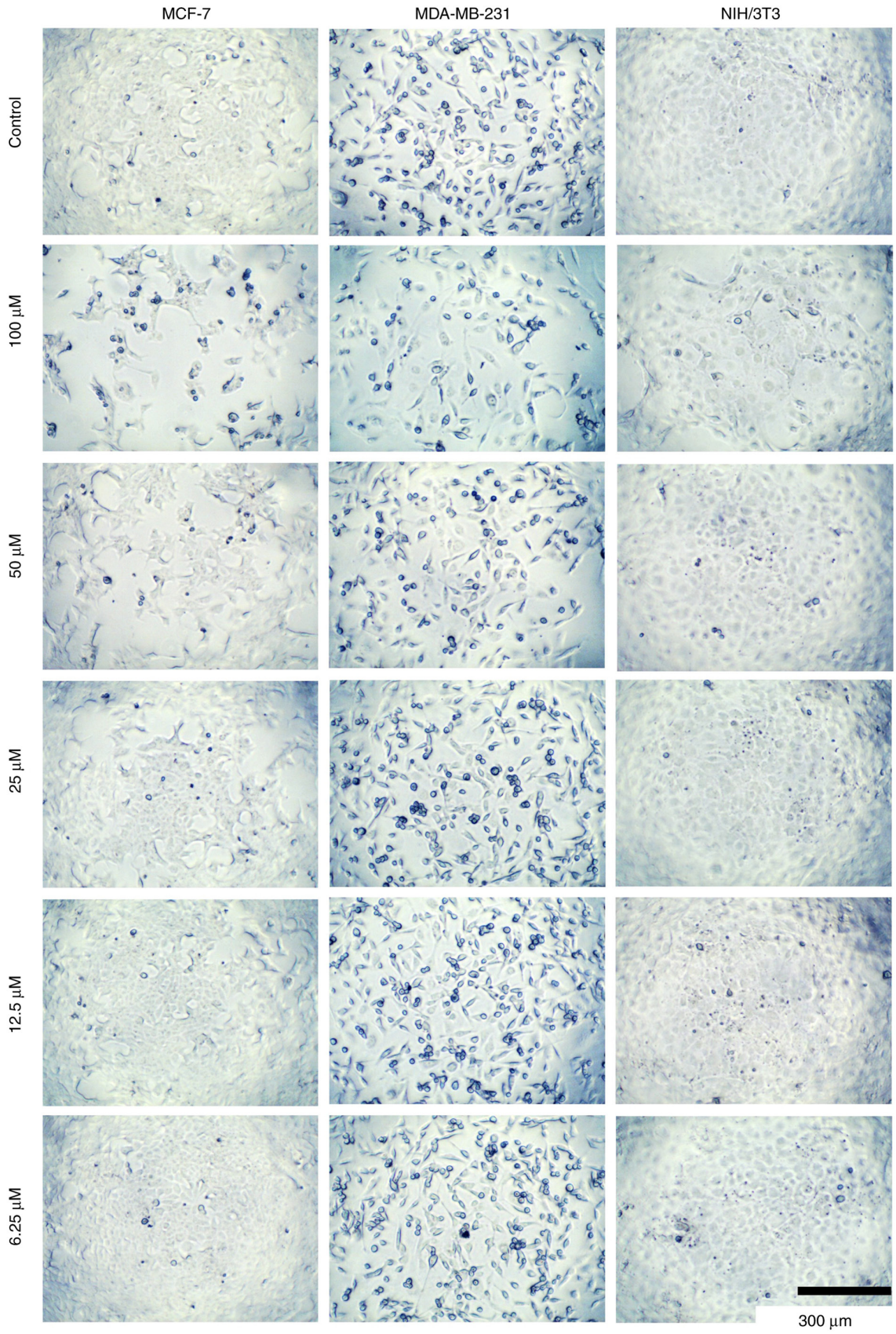

Figure 6. Morphological changes (magnification, x10) in MCF-7, MDA-MB-231 and NIH/3T3 incubated with different concentrations of compound 5.

as belinostat, where an increase in the spacer length is ultimately detrimental to cytotoxic activity (44). This similarity raises the possibility that the phenyl ring, combined with a methylene spacer and a sulfonamide group, could be a key structural motif for modulating the biological activity in these kinds of molecules. However, further research is required

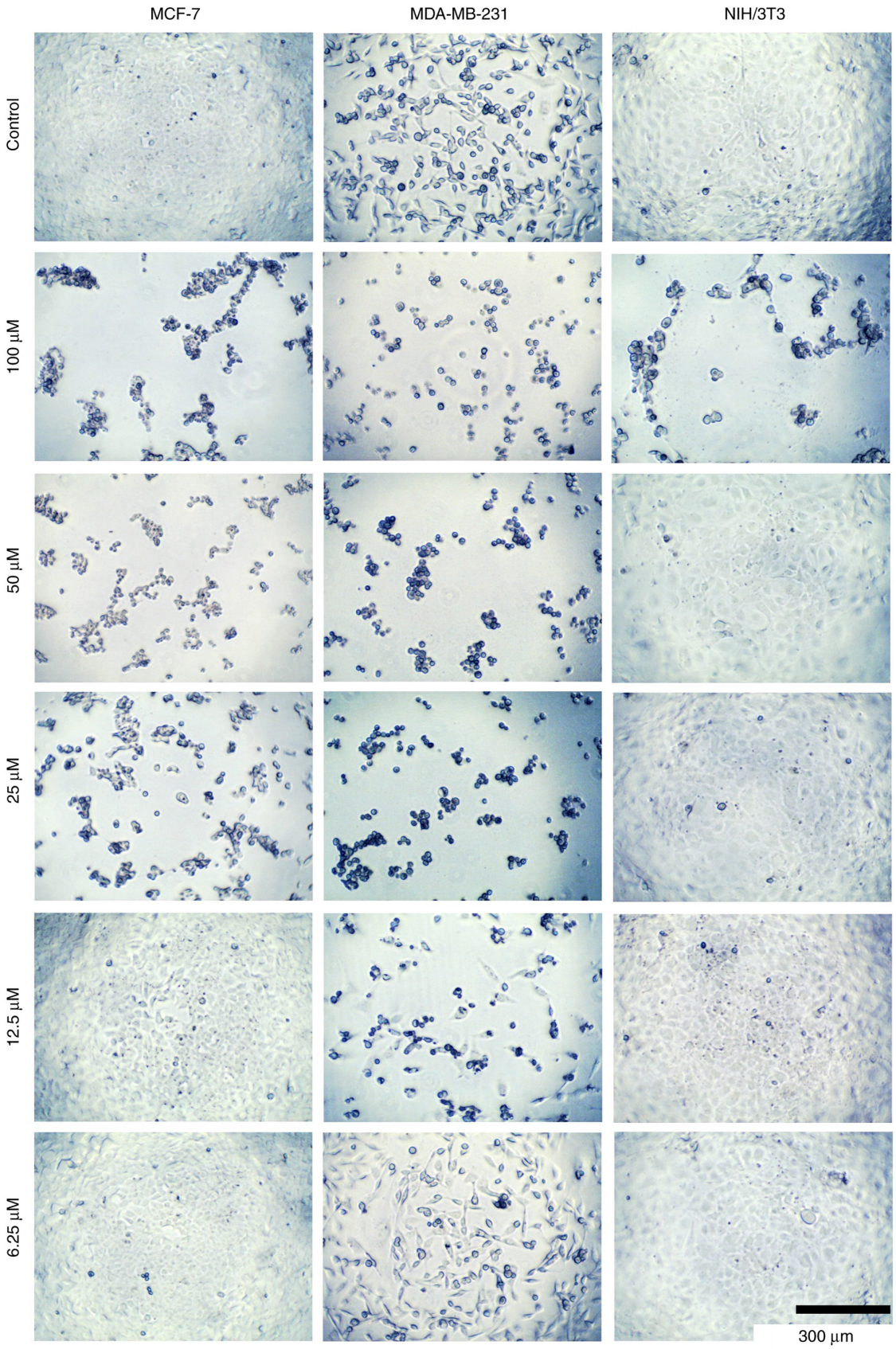

Figure 7. Morphological changes (magnification, x10) in MCF-7, MDA-MB-231 and NIH/3T3 incubated with different concentrations of compound 8b.

to delve deeper into this structural feature, exploring how it influences efficacy and could potentially be optimized for therapeutic use in cancer treatment.

In the present study, it was observed that the belinostat derivatives have significant effects on BC cell lines, but further research is needed to fully elucidate their mechanisms of

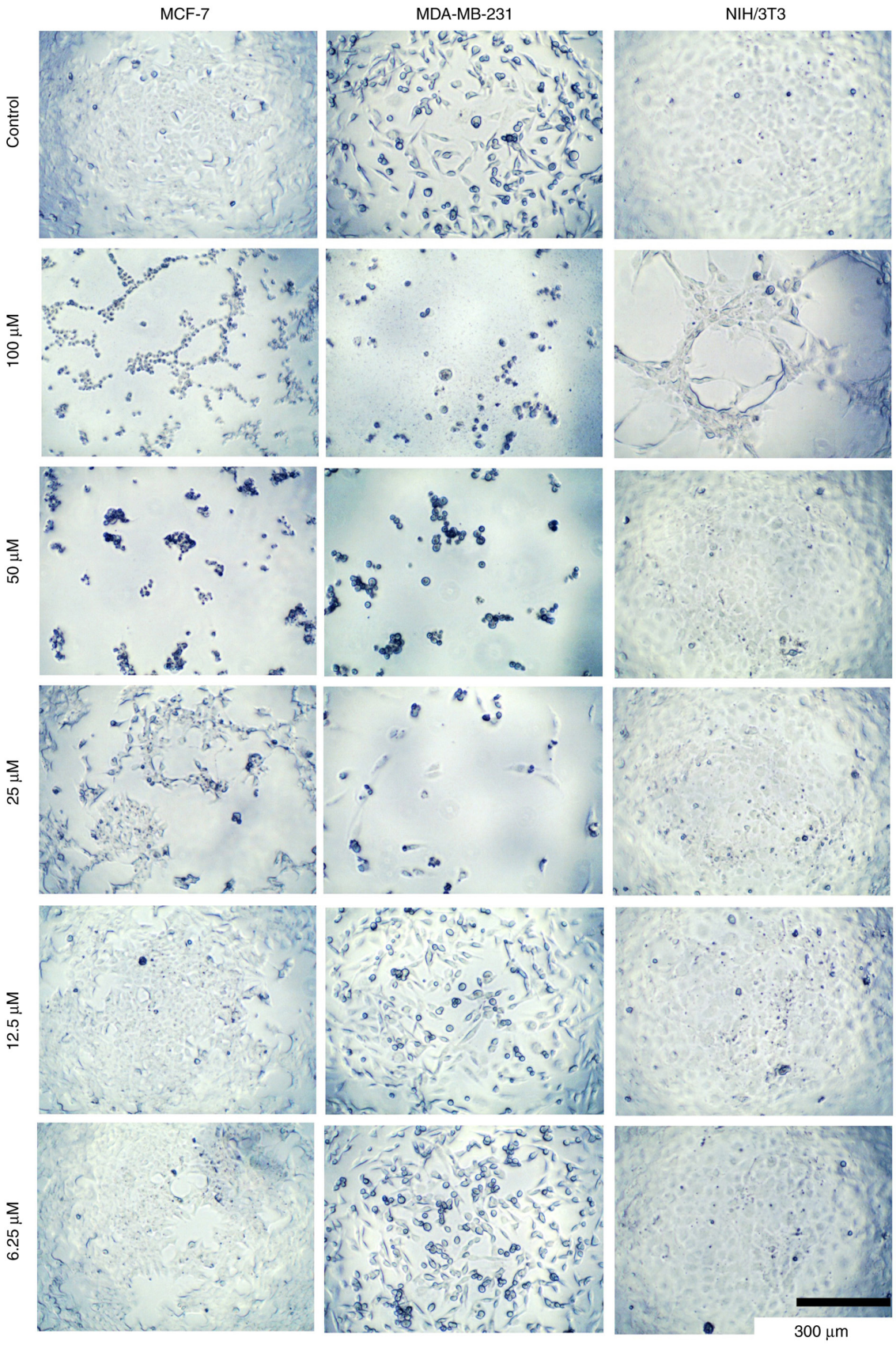

Figure 8. Morphological changes (magnification, x10) in MCF-7, MDA-MB-231 and NIH/3T3 incubated with different concentrations of compound 8c.

action. HDAC6 plays a critical role in BC (45), as it is involved in the invasive behavior of tumor cells and impacts the epithelial organization of HER2-positive BC cells. HDAC6 also deacetylates HMGN2 to regulate STAT5a activity and BC growth (46). Clinical trials have identified that HDAC6 mRNA expression levels can be a prognostic factor and marker of

endocrine responsiveness; patients with HDAC6-positive BC have longer progression-free survival and increased overall survival (46). It is noteworthy that a previous study found that HDAC4, 6, and 8 levels are higher in MDA-MB-231 cells compared with MCF-7 cells (47). This finding aligns with the results of the present study, where the MDA-MB-231 cell line revealed different sensitivities to the compounds compared with MCF-7 cells (Tables II and III). The observed variations in IC_{50} values for the compounds across these cell lines can be partially attributed to the differential expression levels of HDACs. Further exploration of these differences, along with comprehensive physiological, toxicological and morphophysiological evaluations, will be crucial in understanding the full impact of these belinostat derivatives and their potential as therapeutic agents.

Additionally, an experiment was conducted where leukocytes from healthy patients were exposed to the synthesized compounds (4a, 5, 8b, 8c, 4c and 8a) at 40 μM, with belinostat used as a reference (structural core of the compounds). The results indicated that while these compounds demonstrated cytotoxic activity against cancer cell lines, some exhibited slight cytotoxic effects on healthy cells. One compound that demonstrated particularly strong effects was 4a, which exhibited cytotoxic activity of ~84%, making it at least 1.95-fold more cytotoxic than belinostat, with a statistically significant difference ($P<0.05$), indicating its non-selective cytotoxicity across both cancerous and healthy cells. By contrast, compounds 5, 8b, 8c, 4c and 8a exhibited higher viability in leukocytes, with percentages ranging from 73-87%, demonstrating 3-4-fold lower potency than belinostat against healthy cells. Despite this, these compounds maintained strong cytotoxic effects against MDA-MB-231 cancer cells, with statistically significant differences ($P<0.05$, for all comparisons) compared with belinostat. Considering all the aforementioned information, it could be possibly suggested that these compounds may have similar mechanisms of action that allow for selective cytotoxic effects, impacting cancer cells more than healthy cells. The variations in their effects on leukocytes could be related to differences in their chemical structures, such as the presence of methylene spacers and the coumarin system, which might influence their affinity for specific molecular targets. Compound 4a's broad cytotoxicity, while potent, may lack this selectivity, making it less ideal for therapeutic applications where sparing healthy cells is crucial. By contrast, the other compounds' ability to reduce cancer cell viability while preserving a significant proportion of healthy leukocytes suggests a more favorable therapeutic profile, likely due to more selective interactions with their targets. Although this compound appears to exert considerable activity on leukocytes, it would be important in future studies to evaluate its potential in hematological cancer cell lines, as well as to explore other cell lines to fully understand its therapeutic potential.

However, the broad cytotoxicity of compound 4a, while potent, raises the question of whether its mechanism of action could involve pathways beyond HDAC inhibition (45,46), possibly affecting other cellular targets. To further understand the potential therapeutic application of these compounds, it would be interesting to explore whether the observed loss of viability is driven by apoptotic or necrotic mechanisms, as this could significantly influence their safety profile. Additionally, investigating whether these compounds impact other molecular pathways apart from HDACs could reveal broader implications for their use in cancer treatment. These questions highlight the need for more detailed studies to elucidate the precise mechanisms at play and to assess the full therapeutic potential of these compounds.

It is important to acknowledge the limitations of the present study. While various BC cell lines were considered, such as MDA-MB-231 and MCF-7, to enhance the generalizability of the present findings across different BC subtypes, these specific cell lines were chosen due to their distinct levels of HDAC6, a critical factor in the activity of the compounds studied. Although other BC cell lines could be relevant for similar research, the comparison against HDAC6 levels in MDA-MB-231 and MCF-7 cells was central to the focus of the current study. In future research, the authors plan to evaluate additional BC cell lines, including MCF-10A, which is widely used as a model in toxicity studies due to its structural similarity to the normal human mammary epithelium (48,49), to provide a more comprehensive understanding of the compounds' effects.

Another point to discuss is the choice of chemotherapeutics employed. Additionally, cell cycle flow cytometric analysis will be also included in future experiments to evaluate HDAC inhibitors, including the belinostat derivatives. This additional analysis will help to understand the mechanisms by which these compounds affect cell cycle regulation and include detailed evaluations of physiological, toxicological and morphophysiological parameters.

The primary goal of the present study was to assess whether the belinostat derivatives could enhance biological activity compared with existing chemotherapeutic agents. To this end, belinostat, doxorubicin and cisplatin were used in our experiments. Belinostat served as a reference for comparing the biological effects of the derivatives, doxorubicin was included as a standard compound commonly used in Mexico (50,51), and cisplatin was selected due to its extensive use and demonstrated efficacy in numerous studies (52,53), particularly in the context of BC treatments in Mexico (50). Future experiments will also aim to evaluate the effects of other chemotherapeutics, such as carboplatin and oxaliplatin, among others, to provide a more comprehensive overview of the effects of belinostat derivatives and their potential to enhance biological activity. Additionally, animal experiments will be also considered in future studies to verify the effect of drug action *in vivo*, which will help increase the reliability of the research results.

In conclusion, the synthesis, biological evaluation and molecular docking studies of 3-carboxy-coumarin sulfonamides have provided compelling evidence of their potential as effective HDAC inhibitors, particularly targeting HDAC6. The present study revealed that structural features, such as the presence and length of methylene spacers and the incorporation of coumarin systems, are crucial in modulating cytotoxic activity. Molecular docking results showed strong interactions within the HDAC6 catalytic site, with aromatic π-π interactions playing a significant role. These interactions not only align with the observed cytotoxic profiles but also offer insights into further optimization of these compounds. By focusing on enhancing these

structural elements, there is substantial potential to develop more potent and selective HDAC inhibitors, which could become valuable tools in cancer therapy. This comprehensive approach, integrating synthesis, biological testing and computational studies, paves the way for the rational design of next-generation anticancer agents, ensuring both effectiveness and specificity.

Acknowledgements

The authors would like to thank Professor Julio V. Barrios Nuñez from the University of Colima (Colima, Mexico) for their assistance with English language editing.

Funding

The present study was supported by SIP-IPN (grant no. 20241669) and the University of Colima and CONACYT (grant no CVU 514536).

Availability of data and materials

The data generated in the present study may be found in the Figshare platform under accession number 26999875.v2 or at the following URL: https://doi.org/10.6084/m9.figshare.26999875.v2.

Authors' contributions

FJMM, IIPM and JLMA conceptualized the study. JLMA, GAHF, HPD, MOV and ACL developed methodology. ASEG performed software analysis. IDE validated data. JLMA, ACL, HPD and FJM conducted formal analysis. GAHF, IIPM and FJMM performed investigation. FJMM, IDE, IIPM and HPD provided resources. FJMM curated data, performed visualization and project administration. JLMA, GAHF and ACL wrote the original draft. GAHF, FJMM and IIPM wrote, reviewed and edited the manuscript. FJMM and IIPM supervised the study. IDE, FJMM and IIPM confirm the authenticity of all the raw data. All authors read and approved the final version of the manuscript.

Ethics approval and consent to participate

The present study was approved by the Ethics Committee of the Clinical Research Center of the National Cancer Institute (approval no. CEICANCL23062023-DISULFA-21; Colima, Mexico). Cells were isolated from three healthy male volunteer donors, all of whom provided oral informed consent for the collection of their samples. The donors were aged between 26-27 years, with no history of drug use or medication intake 72 h prior to the sample collection.

Patient consent for publication

Not applicable.

Competing interests

The authors declare that they have no competing interests.

Authors' information

JLMA,0009-0002-9367-9069;GAHF,0000-0003-4685-3095; HPD, 0000-0002-4375-6217; MOV, 0000-0003-2052-201X; IIPM, 0000-0002-9645-2049; ACL, 0000-0002-2549-4823; ASEG, 0009-0001-2487-7697; IDE, 0000-0001-9848-862X; FJMM, 0000-0001-6951-9837.

References

1. Lüönd F, Tiede S and Christofori G: Breast cancer as an example of tumour heterogeneity and tumour cell plasticity during malignant progression. Br J Cancer 125: 164-175, 2021.
2. Akram M, Iqbal M, Daniyal M and Khan AU: Awareness and current knowledge of breast cancer. Biol Res 50: 33, 2017.
3. van den Boogaard WMC, Komninos DSJ and Vermeij WP: Chemotherapy side-effects: Not All DNA damage is equal. Cancers (Basel) 14: 627, 2022.
4. Eckschlager T, Plch J, Stiborova M and Hrabeta J: Histone deacetylase inhibitors as anticancer drugs. Int J Mol Sci 18: 1414, 2017.
5. Ružić D, Đoković N, Nikolić K and Vujić Z: Medicinal chemistry of histone deacetylase inhibitors. Arh Farm 71: 73-100, 2021.
6. Yang H, Salz T, Zajac-Kaye M, Liao D, Huang S and Qiu Y: Overexpression of histone deacetylases in cancer cells is controlled by interplay of transcription factors and epigenetic modulators. FASEB J 28: 4265-4279, 2014.
7. Sakamoto KM and Aldana-Masangkay GI: The role of HDAC6 in cancer. J Biomed Biotechnol 2011: 875824, 2011.
8. Matthews GM, Newbold A and Johnstone RW: Intrinsic and extrinsic apoptotic pathway signaling as determinants of histone deacetylase inhibitor antitumor activity. Adv Cancer Res 116: 165-197, 2012.
9. Bondarev AD, Attwood MM, Jonsson J, Chubarev VN, Tarasov VV and Schiöth HB: Recent developments of HDAC inhibitors: Emerging indications and novel molecules. Br J Clin Pharmacol 87: 4577-4597, 2021.
10. Campbell P and Thomas CM: Belinostat for the treatment of relapsed or refractory peripheral T-cell lymphoma. J Oncol Pharm Pract 23: 143-147, 2017.
11. El Omari N, Bakrim S, Khalid A, Albratty M, Abdalla AN, Lee LH, Goh KW, Ming LC and Bouyahya A: Anticancer clinical efficiency and stochastic mechanisms of belinostat. Biomed Pharmacother 165: 115212, 2023.
12. Han XL, Du J, Zheng YD, Dai JJ, Lin SW, Zhang BY, Zhong FB, Lin ZG, Jiang SQ, Wei W and Fang ZY: CXCL1 clone evolution induced by the HDAC inhibitor belinostat might be a favorable prognostic indicator in triple-negative breast cancer. Biomed Res Int 2021: 5089371, 2021.
13. Tuncer Z, Kurar E and Duran T: Investigation of the effect of belinostat on MCF-7 breast cancer stem cells via the Wnt, Notch, and Hedgehog signaling pathway. Saudi Med J 45: 121-127, 2024.
14. Tuncer Z, Duran T, Gunes C and Kurar E: Apoptotic effect of belinostat (PXD101) on MCF-7 cancer cells. Ann Med Res 28: 941-945, 2021.
15. Lu P, Gu Y, Li L, Wang F, Yang X and Yang Y: Belinostat suppresses cell proliferation by inactivating Wnt/β-catenin pathway and promotes apoptosis through regulating PKC pathway in breast cancer. Artif Cells Nanomed Biotechnol 47: 3955-3960, 2019.
16. Stefanachi A, Leonetti F, Pisani L, Catto M and Carotti A: Coumarin: A natural, privileged and versatile scaffold for bioactive compounds. Molecules 23: 250, 2018.
17. Flores-Morales V, Villasana-Ruíz AP, Garza-Veloz I, González-Delgado S and Martinez-Fierro ML: Therapeutic effects of coumarins with different substitution patterns. Molecules 28: 2413, 2023.
18. Yang F, Zhao N, Song J, Zhu K, Jiang CS, Shan P and Zhang H: Design, synthesis and biological evaluation of novel coumarin-based hydroxamate derivatives as histone deacetylase (Hdac) inhibitors with antitumor activities. Molecules 24: 2569, 2019.
19. Balbuena-Rebolledo I, Rivera-Antonio AM, Sixto-López Y, Basurto J, Rosales-Hernández MC, Mendieta-Wejebe JE, Martínez-Martínez FJ, Olivares-Corichi IM, García-Sánchez JR, Guevara-Salazar JA, *et al*: Dihydropyrazole-carbohydrazide derivatives with dual activity as antioxidant and anti-proliferative drugs on breast cancer targeting the HDAC6. Pharmaceuticals (Basel) 15: 690, 2022.

20. Calderón-Segura ME, Gómez-Arroyo S, Villalobos-Pietrini R, Martínez-Valenzuela C, Carbajal-López Y, Calderón-Ezquerro Mdel C, Cortés-Eslava J, García-Martínez R, Flores-Ramírez D, Rodríguez-Romero MI, *et al*: Evaluation of genotoxic and cytotoxic effects in human peripheral blood lymphocytes exposed in vitro to neonicotinoid insecticides news. J Toxicol 2012: 612647, 2012.
21. Hernández-Fuentes GA, Delgado-Enciso I, Enríquez-Maldonado IG, Delgado-Machuca JJ, Zaizar-Fregoso S, Hernandez-Rangel AE, Garcia-Casillas AC, Guzman-Esquivel J, Rodriguez-Sanchez IP, Martinez-Fierro ML, *et al*: Antitumor effects of annopurpuricin A, an acetogenin from the roots of annona purpurea. Rev Bras Farmacogn 34: 111-121, 2024.
22. Haji Agha Bozorgi A and Zarghi A: Search for the pharmacophore of histone deacetylase inhibitors using pharmacophore query and docking study. Iran J Pharm Res 13: 1165-1172, 2014.
23. Zagni C, Citarella A, Oussama M, Rescifina A, Maugeri A, Navarra M, Scala A, Piperno A and Micale N: Hydroxamic acid-based histone deacetylase (HDAC) inhibitors bearing a pyrazole scaffold and a cinnamoyl linker. Int J Mol Sci 20: 945, 2019.
24. Zhang JH, Mottamal M, Jin HS, Guo S, Gu Y, Wang G and Zhao LM: Design, synthesis and evaluation of belinostat analogs as histone deacetylase inhibitors. Future Med Chem 11: 2765-2778, 2019.
25. Shen S and Kozikowski AP: Why hydroxamates may not be the best histone deacetylase inhibitors-what some may have forgotten or would rather forget? ChemMedChem 11: 15-21, 2016.
26. Zhang L, Zhang J, Jiang Q, Zhang L and Song W: Zinc binding groups for histone deacetylase inhibitors. J Enzyme Inhib Med Chem 33: 714-721, 2018.
27. Vickers CJ, Olsen CA, Leman LJ and Ghadiri MR: Discovery of HDAC inhibitors that lack an active site Zn(2+)-binding functional group. ACS Med Chem Lett 3: 505-508, 2012.
28. Traoré MDM, Zwick V, Simoles-Pires CA, Nurisso A, Issa M, Cuendet M, Maynadier M, Wein S, Vial H, Jamet H and Wong YS: Hydroxyl ketone-based histone deacetylase inhibitors to gain insight into class I HDAC selectivity versus that of HDAC6. ACS Omega 2: 1550-1562, 2017.
29. Yu W, Liu J, Clausen D, Yu Y, Duffy JL, Wang M, Xu S, Deng L, Suzuki T, Chung CC, *et al*: Discovery of zthyl ketone-based highly selective HDACs 1, 2, 3 inhibitors for HIV latency reactivation with minimum cellular potency serum shift and reduced hERG activity. J Med Chem 64: 4709-4729, 2021.
30. Osko JD and Christianson DW: Structural basis of catalysis and inhibition of HDAC6 CD1, the enigmatic catalytic domain of histone deacetylase 6. Biochemistry 58: 4912-4924, 2019.
31. Lobera M, Madauss KP, Pohlhaus DT, Wright QG, Trocha M, Schmidt DR, Baloglu E, Trump RP, Head MS, Hofmann GA, *et al*: Selective class IIa histone deacetylase inhibition via a nonchelating zinc-binding group. Nat Chem Biol 9: 319-325, 2013.
32. Butler KV, Kalin J, Brochier C, Vistoli G, Langley B and Kozikowski AP: Rational design and simple chemistry yield a superior, neuroprotective HDAC6 inhibitor, tubastatin A. J Am Chem Soc 132: 10842-10846, 2010.
33. Sixto-López Y, Gómez-Vidal JA, de Pedro N, Bello M, Rosales-Hernández MC and Correa-Basurto J: Hydroxamic acid derivatives as HDAC1, HDAC6 and HDAC8 inhibitors with antiproliferative activity in cancer cell lines. Sci Rep 10: 10462, 2020.
34. Osko JD and Christianson DW: Structural determinants of affinity and selectivity in the binding of inhibitors to histone deacetylase 6. Bioorg Med Chem Lett 30: 127023, 2020.
35. Villa-Martínez CA, Magaña-Vergara NE, Rodríguez M, Mojica-Sánchez JP, Ramos-Organillo ÁA, Barroso-Flores J, Padilla-Martínez II and Martínez-Martínez FJ: Synthesis, optical characterization in solution and solid-state, and DFT calculations of 3-acetyl and 3-(1'-(2'-phenylhydrazono) ethyl)-coumarin-(7)-substituted derivatives. Molecules 27: 3677, 2022.
36. Martínez-Martínez FJ, Padilla-Martínez II and Trujillo-Ferrara J: ^{1}H and ^{13}C NMR assignments of 2-oxo-2H-1-benzopyran-3-acyl and -3-amide derivatives. Magn Reson Chem 39: 765-767, 2001.
37. García-Báez EV, Martínez-Martínez FJ, Höpfl H and Padilla-Martínez II: π-Stacking Interactions and CH···X (X=O, Aryl) hydrogen bonding as directing features of the supramolecular self-association in 3-carboxy and 3-amido coumarin derivatives. Cryst Growth Des 3: 35-45, 2003.
38. Shen S and Kozikowski AP: A patent review of histone deacetylase 6 inhibitors in neurodegenerative diseases (2014-2019). Expert Opin Ther Pat 30: 121-136, 2020.
39. Vögerl K, Ong N, Senger J, Herp D, Schmidtkunz K, Marek M, Müller M, Bartel K, Shaik TB, Porter NJ, *et al*: Synthesis and biological investigation of phenothiazine-based benzhydroxamic acids as selective histone deacetylase 6 inhibitors. J Med Chem 62: 1138-1166, 2019.
40. Campiani G, Cavella C, Osko JD, Brindisi M, Relitti N, Brogi S, Saraswati AP, Federico S, Chemi G, Maramai S, *et al*: Harnessing the role of HDAC6 in idiopathic pulmonary fibrosis: Design, synthesis, structural analysis, and biological evaluation of potent inhibitors. J Med Chem 64: 9960-9988, 2021.
41. Saraswati AP, Relitti N, Brindisi M, Osko JD, Chemi G, Federico S, Grillo A, Brogi S, McCabe NH, Turkington RC, *et al*: Spiroindoline-capped selective HDAC6 inhibitors: Design, synthesis, structural analysis, and biological evaluation. ACS Med Chem Lett 11: 2268-2276, 2020.
42. Xu Y, Tang H, Xu Y, Guo J, Zhao X, Meng Q and Xiao J: Design, synthesis, bioactivity evaluation, crystal structures, and in silico studies of new α-amino amide derivatives as potential histone deacetylase 6 inhibitors. Molecules 27: 3335, 2022.
43. Takla FN, Bayoumi WA, El-Messery SM and Nasr MNA: Developing multitarget coumarin based anti-breast cancer agents: Synthesis and molecular modeling study. Sci Rep 13: 13370, 2023.
44. Sodji QH, Kornacki JR, McDonald JF, Mrksich M and Oyelere AK: Design and structure activity relationship of tumor-homing histone deacetylase inhibitors conjugated to folic and pteroic acids. Eur J Med Chem 96: 340-359, 2015.
45. Zhang Z, Yamashita H, Toyama T, Sugiura H, Omoto Y, Ando Y, Mita K, Hamaguchi M, Hayashi S and Iwase H: HDAC6 expression is correlated with better survival in breast cancer. Clin Cancer Res 10: 6962-6968, 2004.
46. Rey M, Irondelle M, Waharte F, Lizarraga F and Chavrier P: HDAC6 is required for invadopodia activity and invasion by breast tumor cells. Eur J Cell Biol 90: 128-135, 2011.
47. Park SY, Jun JA, Jeong KJ, Heo HJ, Sohn JS, Lee HY, Park CG and Kang J: Histone deacetylases 1, 6 and 8 are critical for invasion in breast cancer. Oncol Rep 25: 1677-1681, 2011.
48. Vale N, Silva S, Duarte D, Crista DMA, Pinto da Silva L and Esteves da Silva JCG: Normal breast epithelial MCF-10A cells to evaluate the safety of carbon dots. RSC Med Chem 12: 245-253, 2020.
49. Paine TM, Soule HD, Pauley RJ and Dawson PJ: Characterization of epithelial phenotypes in mortal and immortal human breast cells. Int J Cancer 50: 463-473, 1992.
50. United Mexican States and General Health Council: 2018 Edition of the Basic Framework and Catalogue of Medicines. Official Journal of the Federation, Mexico, 2018 (In Spanish). https://www.dof.gob.mx/nota_detalle.php?codigo=5544613&fecha=23/11/2018#gsc.tab=0.
51. Jasso L, Lifshitz A, Arrieta O, Burgos R, Campillo C, Celis MÁ, de la Llata M, Domínguez J, Halabe J, Islas S, *et al*: Importance of the list of essential medicines in medical prescription. Gac Med Mex 156: 598-599, 2020.
52. Romani AMP: Cisplatin in cancer treatment. Biochem Pharmacol 206: 115323, 2022.
53. Nauta IH, Klausch T, van de Ven PM, Hoebers FJP, Licitra L, Poli T, Scheckenbach K, Brakenhoff RH, Berkhof J and René Leemans C: The important role of cisplatin in the treatment of HPV-positive oropharyngeal cancer assessed by real-world data analysis. Oral Oncol 121: 105454, 2021.